AT&T Technical Journal
Vol. 64, No. 3, March 1985
Printed in U.S.A.

1.3-μm Laser Reliability Determination for Submarine Cable Systems

By B. W. HAKKI, P. E. FRALEY, and T. F. ELTRINGHAM*

(Manuscript received June 25, 1984)

To meet the stringent requirements of a submarine cable system, our 1.3-μm laser prequalification program has two objectives—first, to define the testing methodology that will accurately evaluate the potential reliability of the laser; and second, to obtain a preliminary indication of laser reliability on which the system configuration can be designed. Our testing methodology involves a combination of step-temperature, step-power, and isothermal testing over the temperature interval between 10 and 80°C and power levels of 1 to 5 mW per facet. Our results show that the long-term degradation process is thermally accelerated, with a median activation energy of 1 eV and a standard deviation of 0.13 eV. By using these activation energies, in conjunction with our measurements of degradation rates, we can project laser performance to 10°C, i.e., system operating temperature. It is estimated that the median time to failure for "light bulb" operation at 10°C is over 2×10^7 hours; and with 98-percent probability it is greater than 5×10^6 hours. Hence, when viewed strictly in terms of light bulb sources of stimulated power, these 1.3-μm lasers have adequate life. In addition, other potential operational malfunctions are being investigated, and they do not seem to change our basic conclusion about the usefulness of these 1.3-μm lasers for submarine cable application.

I. INTRODUCTION

The submarine cable system requires a unique approach to reliability. Each component is subjected to an investigation that (preferably) uncovers the basic failure mechanism(s) and certainly quantifies its

* Authors are employees of AT&T Bell Laboratories.

projected failure probability over the system life. The higher the expected failure rate of a type of component, the greater is the need to accurately predict individual component lives. The reasons are obviously economic: A high failure rate may require a system configuration that utilizes redundancy and increases the initial cost. Furthermore, accurate projections of failures affect system planning to avoid costly undersea repairs. Therefore, the tie between reliability and cost manifests itself in the submarine cable system as in no terrestrial system.

The Buried-Heterostructure (BH), InGaAsP, 1.3-μm laser* considered for use in the optical submarine cable system is the product of a new technology.[1-3] Hence, the primary objective of this prequalification program is to make a preliminary determination of the extent to which the reliability of this 1.3-μm laser satisfies the stringent requirements of the submarine cable system. The program concentrates on the projection of 1.3-μm laser performance to 10°C, which is the system operating temperature. To accomplish this, a significant portion of our effort is devoted to the following: (1) the determination of activation energy(s) that governs the thermally accelerated mechanism(s); (2) the aging law that describes the time evolution of current at a specific temperature; (3) the projection of performance to the system operating temperature of 10°C; and, concurrently, (4) the identification of the dominant failure mechanism(s) that will determine the life of the laser.

Our laser prequalification program is diversified in such a manner as to provide extensive information about the various facets of laser performance. Thus, we use two generically different testing methodologies: step stress and isothermal.[4] The two methods provide supportive, complementary, and corroborative information that is essential to a better understanding of laser reliability. For example, isothermal tests provide useful information about the time dependence of the aging law, end-of-life criteria, activation energy, and data that validate the assumptions made in step-stress analysis. On the other hand, step-stress tests provide an efficient measure (in time and number of devices) of the activation energy, degradation rates, and the dependence of these rates on optical power. These two programs will be described in detail, and test results will be given on 262 unpurged[5] lasers, wherein the accumulated time (as of February 1984) is $\sim 2.4 \times 10^6$ device hours. (The lasers were comprised of early vintage [1980–2] devices that had seen two types of burn-in screen. The

* The laser chip investigated is made by Hitachi Ltd. and meets AT&T Bell Laboratories specifications. The buried active region is nominally 1 to 1.7 μm wide, 0.1 to 0.3 μm thick, and 300 μm long. The laser is subsequently packaged within AT&T.

majority of lasers were burned in at 50°C/5 mW/100h, at constant current, and met the condition that the power change was less than 10 percent. The rest of the devices were burned in at 60°C/5 mW/100h, at constant power, and satisfied the condition that the drive current increased by less than 5 percent.) The projections given here are based on the assumption that there will be no unexpected device failures, such as those due to weakly temperature-activated mechanisms. Data needed to estimate the sudden failure rate of the lasers are also collected in this prequalification program. A separate purge program is expected to eliminate such devices.[5]

This paper is organized as follows:

II. 1.3-μm LASER RELIABILITY

2.1 Failure modes

A laser can fail either as a "light bulb" or operationally in a transmitter. A light bulb failure is defined as the inability of the laser to deliver the requisite amount of stimulated power (e.g., 5 mW/facet) within the constraints of the current available for the transmitter. On the other hand, there are more stringent operational requirements imposed by the transmitter. These pertain to the ability of the laser to provide the quality of optical signal that is required to maintain an error rate below a certain value (e.g., 10^{-9} per bit).[6] Light bulb failure, due to an increase in the drive current at a fixed optical power, can be due to an increase in threshold of the active region, a decrease in the differential quantum efficiency, an increase in extraneous leakage currents,[5] or change in the front/back power ratio. All these parameters are measured, as described in detail in Appendix A. Most of the

present published effort on lasers concentrates on the increase in drive current and its acceleration by temperature, i.e., its activation energy. For reasons to be discussed later, we will present in this paper primarily our results on the degradation of the threshold current. However, our ongoing program is investigating laser operational failures caused by the excitation of high-order transverse modes, spectral splitting,[6] modal partition noise, change in extinction ratio, occurrence of self-induced pulsations, or mechanical instability in the package (see also Appendix A). Except for the degradation of threshold, we presently do not know whether the rest of the potential failure mechanisms are thermally activated. This important question is being addressed as part of the continuing reliability program.

2.2 Testing methodology

There are many different approaches to the prediction of lifetime at operating temperature. These have been described to some extent in the literature.[7] Each method has its own advantages and disadvantages as far as our 1.3-μm laser program is concerned. For our purpose, we have chosen a combination of isothermal and step-stressing methods, which seem to be best suited for our program.

2.2.1 Step-stress testing

Step-stress testing is an efficient method of measuring a fundamental mechanism by holding most parameters constant, but varying one, e.g., temperature or optical power. Since the test is done on each device, it can, in principle, accurately estimate the dependence of the degradation on the parameter(s) that is varied. However, when this methodology is applied to temperature and power-step-stressed lasers, several issues must be resolved in order to achieve a high confidence level in the results. These step-stressed issues are the following: (1) the amount of bias (if any) in the derived quantity, such as activation energy, due to the particular choice of a temperature sequence (temperature reciprocity); (2) the applicability of the observed power-step-stress results obtained at some temperature, to other temperatures; and (3) whether the results obtained at each step-stress test are representative of the dominant long-term degradation process.

At the present stage of the program, we have preliminary answers to the above-mentioned questions. However, the issues raised have, to a large extent, helped in designing the step-stress experiments so that by the conclusion of the qualification program, the majority, if not all of these questions, will be answered.

A total of 117 lasers (see Appendix B) were stepped in temperature and power. The temperature was stepped in the range between 50 and

80°C, and the power was stepped between 1 and 5 mW/facet. By comparing the degradation rates of threshold current at different temperatures, but at constant power, a measure of activation energy for this parameter was obtained. Similarly, by holding the temperature constant, but changing the optical power, we obtained the dependence of the degradation rate on the level of operation. Our step-stressing methodology subscribed to the following guidelines:

1. The degradation rate of threshold at constant power level was determined at three different temperatures, T_1, T_2, and T_3.
2. The degradation rate was determined at constant temperature, but at several power levels, i.e., 1, 3, and 5 mW/facet.
3. At each test condition, the average increase in drive current was kept within the range of a minimum of ≈5 percent and a maximum of ≈25 percent, at the end of the first test interval (15-percent maximum for subsequent intervals).
4. In each group of lasers being tested, a minimum of five lasers from a particular slice was used, if possible, as indicated in Appendix B.
5. A laser was considered (arbitrarily) to have reached the limit of its light bulb life when the threshold current increased by 100 percent.

The first guideline provided information needed to derive the activation energy(s). At face value, it might seem simple and straightforward. However, to make a valid extrapolation from (T_1, T_2, T_3) to the operating temperature at 10°C, certain requirements must be satisfied. These are (1) a single activation energy for threshold current degradation applies for all four temperatures: T_1, T_2, T_3, and 10°C; (2) the dominant aging mechanism is an extrapolatable function of time at all temperatures (predominantly linear behavior is observed); (3) the results are independent of the chosen sequence of temperature (temperature reciprocity); and (4) the same degradation mechanisms exist at all temperatures but at different rates. All these requirements are currently under investigation, and isothermal testing should provide useful and corroborative information.

The second guideline was motivated by the fact that since some of these BH lasers, for a number of reasons, could not deliver 5 mW at 80°C, we had to lower the power level to 3 mW. The difference in aging rates at constant temperature, but at different power levels, was determined in order to evaluate the impact of the level of operation on the degradation rate, as well as to identify the primary driving mechanism that controls degradation.

In the third guideline, the maximum allowed change was imposed to retain enough life in a laser to undergo subsequent testing at different temperatures or powers. The minimum change of 5 percent was needed to produce changes in the laser that were physically

significant, amenable to analysis, and to ascertain, to the extent possible, that a linear degradation rate was in fact applicable.

The fourth guideline was required for statistical significance. The wide variations observed in the values of degradation rates among various slices prior to purging preclude accurate analysis when performed on randomly selected lasers, at least within the sample sizes of 20 or 40 per test. Instead, the experiments were designed to distribute lasers from the same slice over the various test conditions to better account for slice-to-slice variability. Finally, the last guideline was somewhat arbitrary. It is conceivable that lasers may increase in threshold current by a factor greater than 100 percent before functionally failing. A more comprehensive determination of the end-of-life condition is being made in the context of operational failures by measuring the error rates of aged lasers operating in transmitters.[6]

Figure 1 shows schematically the temperature and power step stressing that two groups of devices, 20 lasers each, underwent. Group 1, detailed in Appendix B, was initially power step stressed by operating at 5 and 3 mW, consecutively. This was followed by the temperature step stressing indicated in Fig. 1. Group 2 (see also Appendix B) was

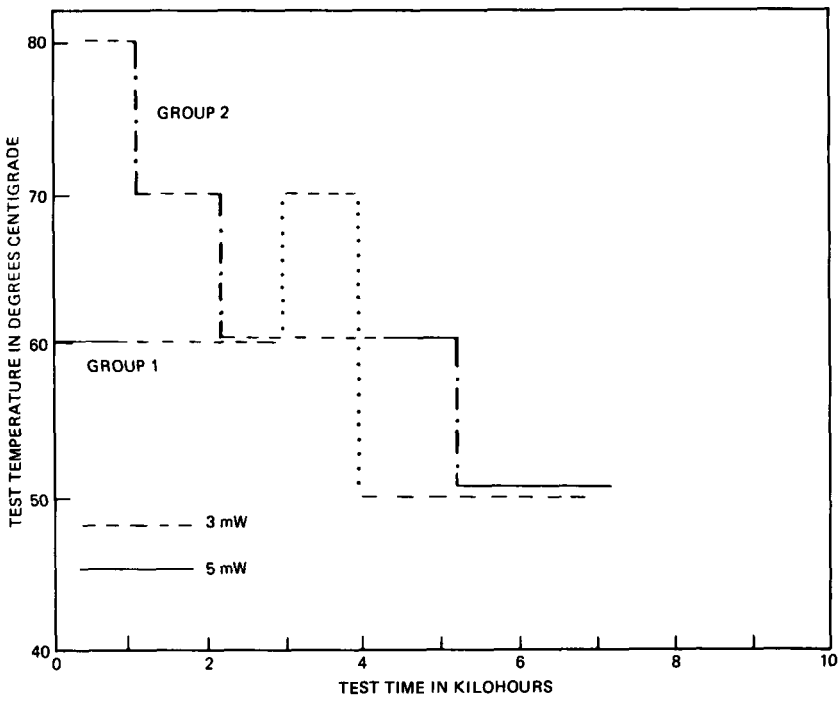

Fig. 1—Sequence of step stressing Groups 1 and 2 in temperature and power. The actual testing is continued beyond 8000 hours (not shown).

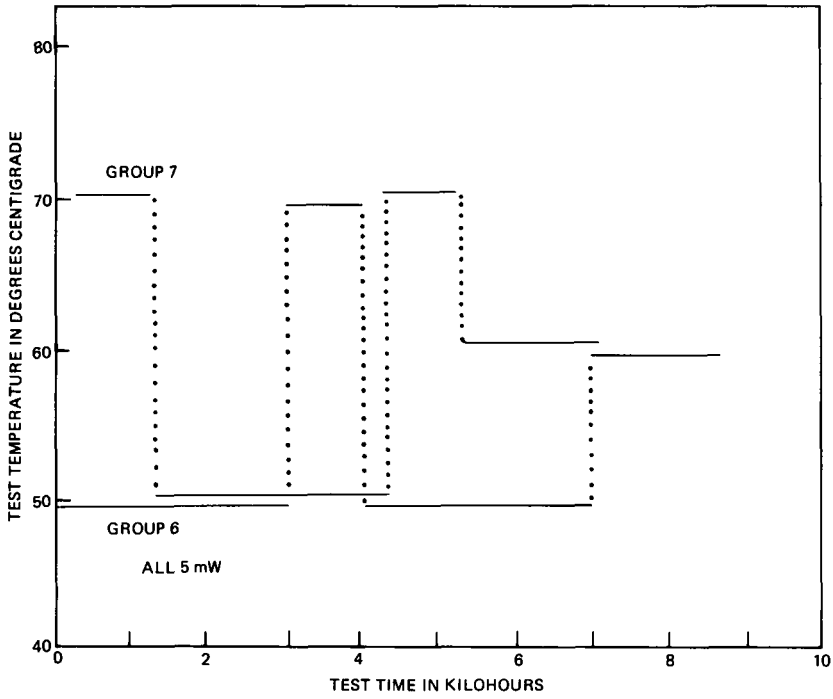

Fig. 2—Sequence of step-temperature testing Groups 6 and 7 at 5 mW per facet.

temperature step stressed by lowering the temperature from 80°C, in 10°C increments, keeping the optical power constant at 3 mW/facet. At 60°C, Group 2 was power step stressed by increasing the power from 3 to 5 mW. The rest of the sequence in Fig. 1 is self-explanatory.

The test sequence of Groups 1 and 2 provided information about activation energy and degradation rate dependence on optical power, in a relatively short period of time. However, the experiment did not provide information about temperature reciprocity, other memory effects, bias in data, etc. For this purpose, two additional groups of devices, 6 and 7, were step stressed in temperature, as shown schematically in Fig. 2. These two groups were selected and tested with the following considerations in mind: (1) The two populations were "alike" in the sense that the lasers used came from the same slices of material, to the extent possible (see Appendix B). This resulted in 37 and 40 lasers used in Groups 6 and 7, respectively. (2) The temperature sequences were mirror images of each other, in order to check temperature reciprocity. (3) Three temperatures were used for aging, in an attempt to confirm an Arrhenius relation for the degradation rates. (4) The power was held constant at 5 mW (system operating level) throughout the test, in order to reduce the variance in the results

associated with the dependence of the degradation rate of threshold current on the optical power level.

2.2.2 Isothermal testing

Isothermal testing of two or more groups operating at different temperatures is the more conventional approach to reliability study.[7] Normally, comparing the time-to-failure distribution curves at different temperatures gives the activation energy for the degradation process.[8] To get an accurate estimate of the activation energy by this method, it is necessary to satisfy two requirements: (1) the device population is homogeneous, i.e., device-to-device variability is smaller than the acceleration associated with temperature; and (2) there is adequate testing time available at the respective temperatures to establish the true nature of the failure distribution curves.

Both of the conditions stated above were difficult to fulfill in the case of our 1.3-μm lasers. In the first place, for any sample size of 40 or more unpurged lasers, obtained from several slices, it was not uncommon to see up to three orders of magnitude variation in rates of degradation. This exceeded the expected difference in temperature acceleration, for practical operating temperatures in the range of 40 to 70°C. Secondly, for practical aging temperatures, the failure rate was predicted to be low enough to require an unrealistic length of testing time to establish a failure time distribution curve. This second drawback was circumvented by using isothermal distribution curves of degradation rates instead of failure rates.[3,9,10] This, in turn, raised another problem, namely, the relationship between degradation rate and end-of-life for a device.

Given the respective advantages and disadvantages of step-stress and isothermal testing, we concluded that both methodologies are essential for a well-balanced program. Therefore, we dedicated a total of 145 lasers for isothermal testing at 10, 30, 40, and 60°C, in groups of 40, 25, 40, and 40 lasers, respectively, as described in Appendix B. To the extent possible, we attempted to design the test groups to be alike. That is, we selected slices that provide many lasers and then distributed the lasers from each slice among the various groups to be tested at different temperatures. This minimized the effects of slice-to-slice variability in degradation rate and enhanced our ability to derive an activation energy from the isothermal data. Hence, at a minimum, we expect this isothermal testing program to provide information about the aging law, correlation between degradation rate and time-to-failure, and the evolution of mechanisms that may lead to functional failures.

2.3 Aging law

The aging law governs the time evolution of device current at various

temperatures. When the lasers are operated at system power level (e.g., 5 mW), it is necessary to distinguish between changes in threshold current and those associated with the modulation current (the latter being the difference between threshold and the current at 5 mW per facet). This is done because there is no a priori reason to expect that the same degradation mechanisms apply equally to both current components. In fact, test results suggest that the aging mechanism for threshold may in some cases be different from that for the modulation current. Hence, as a first step in this analysis, the aging law will be obtained for the threshold current.

Our study of 1.3-μm BH lasers has shown that the threshold current shows the following behavior: (1) at constant temperature (isothermal) the current increases with time; (2) at a specific time (isochronal) the threshold increases with temperature; and (3) at a given temperature and time, a temporary disturbance in the operating condition (a momentary change in operating temperature or lasing condition) results in a transient change in the current-time response. These characteristics differ in their strengths and severity from laser to laser. However, their existence requires that both the experiments and the interpretation of the results account for these phenomena, to the extent possible.

An example of the time dependence of the threshold current of a particular laser is shown in Fig. 3a. The device was operated at 60°C and 5 mW/per facet. The threshold current in Fig. 3a was normalized with respect to its initial value. There are several noteworthy features in the data of Fig. 3a. For instance, the current initially increased at a rapid rate during the first 700 hours. This rapid increase ceased beyond 1000 hours; thereafter the current assumed a more moderate rate of increase. The rapid decrease in aging rate at 1000 hours forms what we call the "knee." At 1800 hours, the testing at 60°C was interrupted to measure the laser characteristics at 10°C. After testing was resumed at 60°C, the current beyond 1800 hours showed a small transient. In this particular device the transient was quite moderate in size. Similarly, at 5500 hours the testing was interrupted but the device stayed at 60°C. This again resulted in a small (almost insignificant) transient. Further test data up to 13,100 hours, of the laser shown in Fig. 3, indicate a continuation of the linear "postknee" linear aging behavior.

Other electro-optical measurements shed some light on the effects associated with the knee, also shown in Fig. 3b. In the first place, the magnitude of the saturable current at the knee seemed to be slice dependent. In the second place, the modulation current, as a function of time, often exhibited a knee similar to that associated with the threshold current. Finally, the junction voltage at threshold also

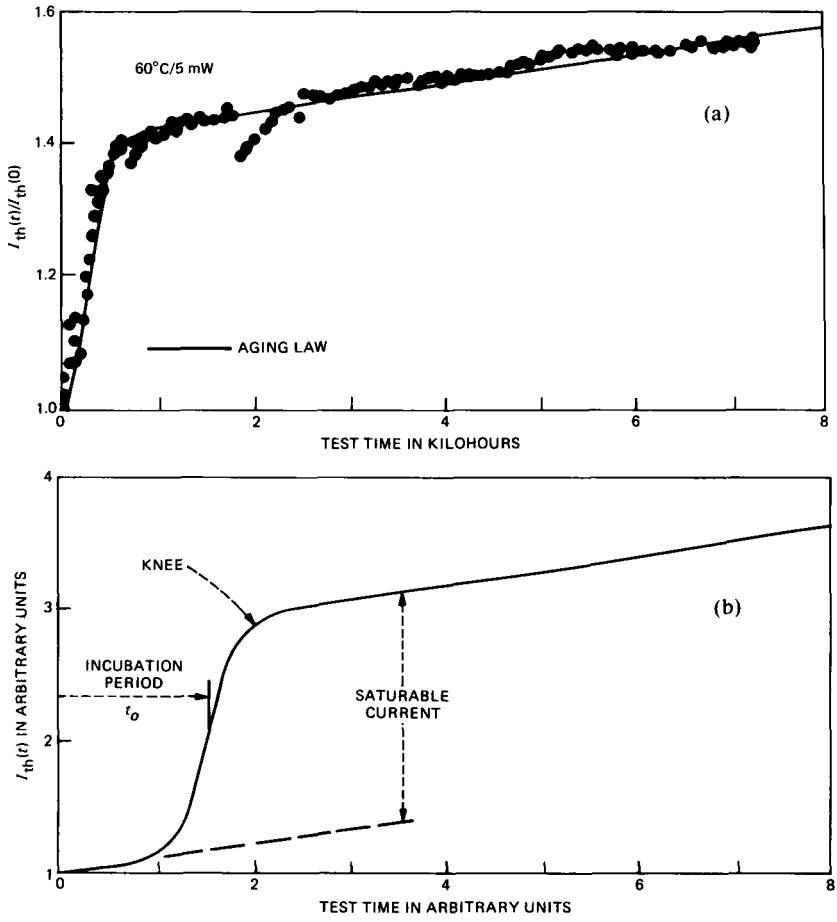

Fig. 3—(a) An example of the change in threshold with time taking place in a laser stressed at 60°C and 5 mW. (b) Schematic representation of the aging behavior of threshold current.

showed a small initial increase (a few millivolts), which saturated beyond the knee. (The junction voltage at threshold is obtained by subtracting from the operating voltage the measured product of threshold current and device resistance.) Hence, the change in threshold current prior to the knee was not an isolated effect.

It is clear that the degradation mechanism(s) in the laser is in fact very complicated. We are not, at the present time, in a position to make unequivocal statements about the fundamental phenomena that are influencing the laser behavior. It is possible, however, to glean from the data information that is suggestive of the basic mechanisms that are active. For this purpose, the aging law for current as a function

of time, an example of which is shown in Fig. 3, is a proper starting place.

The aging law for threshold current can be written in the general form[11]

$$I(t, T') = \left[C + \int_0^t G(t', t, T)dt'\right]F(T'), \tag{1}$$

where C is a constant, and the integral evaluates the increase in current due to degradation, when the device is stressed at some temperature T for a time t. $F(T')$ is an isochronal function that may be the $\exp(T'/T_0)$ expression typically used for lasers, where T_0 is the characteristic temperature.[12-17] Finally, the application of eq. (1) to actual cases requires care. In the first place, the extent of degradation (due to any combination of current, temperature, optical power, etc.) over any time t is evaluated by the integral of eq. (1). In the special case of isothermal aging, the temperature T is held constant over the aging time t. In the second place, when the aging process is halted at any time t, the instantaneous temperature sensitivity of current is accounted for entirely by the isochronal function $F(T')$.

Equation (1) assumes that as the laser degrades, the isochronal dependence of threshold current on temperature, at any time, remains unchanged. Our data indicate that this is usually a valid assumption. To confirm this, we show in Fig. 4 a plot of the measured relative change in threshold current due to aging at T, i.e., $\Delta I(t, T)/I(0, T)$ and the resulting relative change measured at 10°C, $\Delta I(t, 10)/I(0, 10)$. In spite of the obvious scatter in the data points, it is possible to obtain a linear regression analysis that gives

$$\frac{\Delta I}{I}(10°) = (1.027 \mp 0.047)\frac{\Delta I}{I}(T) + 0.064. \tag{2}$$

It is seen from eq. (2) that there is a one-to-one correspondence in the *relative* change in threshold current at various temperatures. The cause of the small residual intercept is uncertain. It could be due to measurement error, transients associated with temperature changes, or a small but finite change at 10°C that deviates from a linear relationship. In any case, it is concluded that for significant changes, aging lasers at one temperature produces the same relative changes in threshold at other temperatures. In other words, the characteristic temperature T_0 of the laser remains nearly the same.

The formalism of the aging law given in eq. (1), in principle, can account for the history of the device through the function G. In other words, at any time and temperature the degradation rate depends on the extent of degradation that took place previously. Although concep-

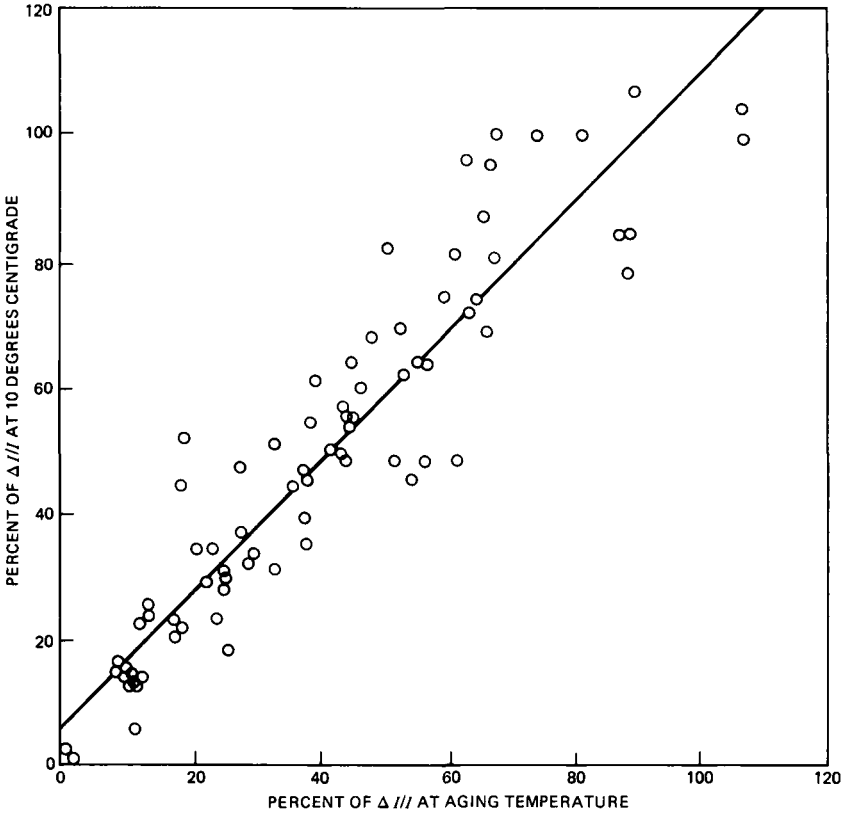

Fig. 4—Correlation between relative changes in threshold incurred at high temperature aging and the corresponding changes measured at 10°C.

tually useful, the integral form will be supplanted by empirical closed-form expressions that can be applied to actual cases. Thus, the isothermal aging law for threshold current can also be written in the form

$$I(t, T') = I_0[I_T^s(t) + I_T'(t)]F(T'), \tag{3}$$

$$I(0, T') = I_0F(T'), \tag{4}$$

where I_0 is a dimensional constant, $I(0, T')$ is the initial value of current at T', $I_T^s(t)$ is a function that accounts for the component of degradation that saturates with time, and $I_T'(t)$ is the nonsaturable long-term degradation function. Finally, in eq. (3) the normalized sum of the functions $[I_T^s(t) + I_T'(t)]$ depends at any time on the thermal aging history of the laser but is not an explicit function of the instantaneous temperature.

A physically reasonable model for the observed saturable current of

Fig. 3 involves diffusion of a nonradiative or optically absorbing center.[9,18] However, a detailed analytical model for such a complicated process is not yet available. We are thus forced to resort to an empirical formulation for the saturable current. After considering a number of analytical expressions, including powers of time, we found the following expression to fit the data best:

$$I_T^s(t) \alpha s\left[1 + \exp\left(\frac{t_0 - t}{\tau}\right)\right]^{-1}, \tag{5}$$

where s is the relative strength of the saturable current, t_0 is the incubation period of the saturable current, shown schematically in Fig. 3b, and τ affects the rate of change of the saturable current at t_0. (In many devices, the saturable current does not appear immediately, but rather takes several hundred hours—depending on the stress temperature—before it occurs, i.e., t_0 varies from laser to laser.) Both time contants t_0 and τ are expected to vary with temperature, as will be discussed in later sections.

Finally, the long-term degradation component $I_T'(t)$ can be described in many ways. The simplest is a linear dependence. Our data on unpurged lasers are consistent with this form, and, in addition, it provides a more conservative approach than the sublinear model. Therefore, we will assume that

$$I_T'(t) \alpha 1 + Rt. \tag{6}$$

The empirical current aging law is obtained by combining eqs. (5) and (6). For the isothermal case and for $T = T'$, we obtain

$$\frac{I(t, T)}{I(0, T)} = \left[1 + Rt + \frac{s}{1 + e^{(t_0 - t)/\tau}}\right] \Big/ N, \tag{7}$$

where

$$N = 1 + s/(1 + e^{t_0/\tau}). \tag{8}$$

N is the normalization constant such that at $t = 0$, $I(t, T)/I(0, T) = 1$, and T is both the aging and measurement temperature.

Figure 3a shows a fit to the data in which $R = 2.2 \times 10^{-5}$ hours^{-1}, $s = 0.46$, $t_0 = 260$ hours, and $\tau = 110$ hours. It is evident that the aging law fits the data. Furthermore, the absence of a clear superlinearity in the long-term aging behavior, in a large number of our unpurged devices, argues against a strong current-driven aging mechanism. Therefore, in the absence of information to the contrary that may be revealed by future testing, the linear model will give us a useful measure of degradation at low temperatures and long times, and will be used in our projections.

2.4 Reliability results

2.4.1 Activation energy

The long-term degradation rate R of threshold current is assumed to obey the Arrhenius relation

$$R = R_0 e^{-E_a/kT}, \tag{9}$$

where R_0 is a constant, E_a is the activation energy, k is Boltzmann's constant, and T is temperature. The activation energy is evaluated in the postknee regime by measuring the function $I'_T(t)$ at two temperatures, T_1 and T_2. Thus, eqs. (6) and (9) give

$$E_a = \frac{kT_1T_2}{T_2 - T_1} \ln\left(\frac{dI'_{T_2}/dt}{dI'_{T_1}/dt}\right). \tag{10}$$

Conversely, the activation energy can be obtained from eq. (7) in the postknee regime, i.e., $t \gg t_0, \tau$ by substituting into eq. (10) the derivatives of the total normalized currents. (This presupposes that t_0 and τ for the saturable current have the same activation energy. However, this activation energy can be different from that for the long-term degradation mode, as will become evident from Section 2.4.2.)

Most of our data presently available on activation energy were obtained from the step-stress experiments of Figs. 1 and 2. Although the step-stress test sequence of Fig. 2 is not complete, a fairly substantial amount of data has already been taken. These data, although preliminary in nature, are considered to be sufficiently accurate to make valid projections to the system operating conditions. The isothermal data, which will be treated statistically separately,[4] will be used as a general corroborative test of the validity of step-stress results.

Presently, the potential number of data points for determining activation energy is 177. This is the result of step-stress testing 117 lasers, as in Figs. 1 and 2. (The amount of data will increase further as the test program proceeds.) Given the myriad factors associated with the current aging behavior that can reduce the accuracy of deriving an activation energy, the useful number of data points was less than the total. The data for activation energy, obtained from step-stress experiments, were screened according to the following criteria:

1. The data were taken in the postknee regime of Fig. 3. This was to ensure that the activation energy was being derived only for that mechanism that governs the long-term wear-out of the device, as would apply for purged devices.[5]

2. The degradation rate at high temperature must be sufficiently low to establish a (nearly) linear degradation rate over a significant (≈500-hour) period of time.

3. The degradation rate at low temperatures must be sufficient (>0.3 percent per kh) to allow an accurate determination of its value (see Appendix A) over a reasonable test interval (3 kh).

4. Devices should not exhibit severe sensitivity to temperature changes—i.e., transients in the aging behavior—during step-temperature testing.

Out of 177 potential data points, only 26 measurements met the above criteria. The activation energies from these measurements are shown in the distribution plot of Fig. 5. In spite of the precautions listed above, there is still a significant spread in the data. This spread is due to a combination of experimental errors and device variations. It is suspected that the former contributed significantly (≈0.1 eV) to the spread of the distribution curve shown in Fig. 5. From the data of Fig. 5, as well as data to be discussed in subsequent sections, a median value of 1 eV for activation energy is reasonable. Figure 5 also indicates that the central 96 percent of the values of activation energy are between 0.76 and 1.28 eV.

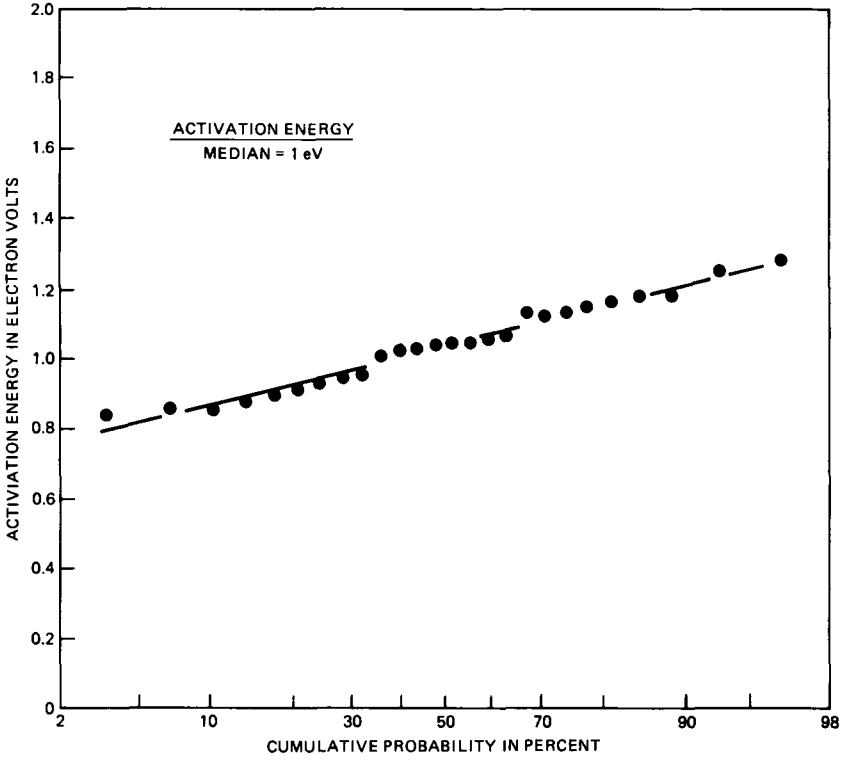

Fig. 5—Distribution curve of activation energy obtained from step-temperature stressing.

Table I—Activation energy and step-stress sequence

Activation Energy (eV)	Temperature Step (°C)					
	80 → 70	70 → 60	60 → 70	70 → 50	50 → 70	40 → 50
Mean	1.09	1.07	0.92	1.07	1.01	0.88
Median	1.02	1.17	0.90	1.10	1.03	0.82
Standard Deviation	0.31	0.33	0.08	0.15	0.31	0.30

Although only 26 measurements of activation energy are presented in Fig. 5, the rest of the data need not be entirely discarded. It can be used in a semiquantitative way to study such effects as temperature reciprocity, the applicability of the Arrhenius relationship, and memory effects. For this purpose, all the data from step-temperature stressing were used, and the results from various test sequences are given in Table I. (Table I also includes the results of step-temperature stressing another group of devices between 40 and 50°C. This is a separate group from those indicated in Figs. 1 and 2.) It is clear from the data that without the application of the guidelines stated above, the standard deviation of the activation energy increased by almost a factor of two. However, the mean and median values were still in the 1-eV range. In addition, two important observations could be made from the results of Table I. First, the mean activation energy, as obtained from the Arrhenius relation, was relatively invariant with temperature over the range of 40 to 80°C. Second, when step-temperature measurements were made in the postknee regime of the current aging characteristic, the derived activation energy showed no significant ($\mp$ 0.1 eV) dependence on the sequence of testing.

The lasers undergoing isothermal testing at 60 and 40°C provided activation energies that corroborated the step-temperature results. However, exact agreement was not possible because the isothermal tests suffered from the following difficulties: (1) With the limited testing time available ($\approx$7000 hours), the 60°C group had device currents that developed well beyond the knee; the 40°C group, with 13,700 hours of testing, still exhibited increased degradation rates associated with the residual saturable current. (2) Prior to screening (to be discussed below), the laser-to-laser variation within a slice and the slice-to-slice variation in the degradation rate exceeded (by approximately two orders of magnitude) the expected difference in degradation rate associated with temperature. (3) The number of devices being tested at each temperature (40 lasers) was probably too small to reduce the expected uncertainty in the activation energy below that derived from step-temperature testing.

To overcome the problems of the second difficulty above, data on five slices (H, I, L, M, and N of Appendix B) that were common to

the two test groups were subjected to a linear regression analysis. In addition, to avoid bias in the results, the following measures were taken: (a) in each slice, if a certain number of lasers (0 to 20 percent) degraded too rapidly at high temperature to provide a meaningful measurement, an equal number, from that slice, of the most rapidly degrading lasers at low temperatures was eliminated; (b) in each slice, if a certain number of lasers (0 to 15 percent) at low temperature were not degrading sufficiently to be accurately measured, then an equal number of the slowest degrading lasers at high temperature were also eliminated from the population. This, in essence, maintained the integrity of the heart of the distributions at both temperatures. The resulting activation energy for all the remaining lasers obtained from the five different slices was 0.79 eV, with a standard deviation of 0.19 eV. This was lower than the median value of 1 eV obtained from step-temperature stress. The reason was probably due to some residual effects of the saturable current in the 40°C data. This was supported by the observation that two of the slices (I and M of Appendix B) had low values of saturable currents. The isothermal data on these two slices, when considered separately, gave an activation energy of 1.0 eV and a standard deviation of 0.25 eV. Hence, it is expected that longer testing at 40°C will give lower degradation rates, as the influence of the saturable current component decreased. This will increase the values of activation energy obtained from isothermal tests and provide a more accurate lower bound on the activation energies. Finally, this analysis of the isothermal data is an alternative to the method of deriving the activation energy used by Amster.[4]

2.4.2 Saturable current

One of the factors that complicated the interpretation of both the step-stress and the isothermal data was the presence of the saturable current. This current manifested itself experimentally as shown in Fig. 3 and was represented analytically by the empirical relation given in eq. (5). Although eq. (5) is strictly empirical, it is a useful tool that provides a quantitative measure of the strength of the saturable current and its rate of formation. Thus, from eq. (5) a critical time t_c is defined by

$$t_c = t_0 + \tau, \tag{11}$$

which is the time required for the saturable current to achieve ≈73 percent of its final value. To obtain an activation energy for the saturable current, the data of the isothermal test groups, operating at 40 and 60°C, were utilized. In addition, the data obtained during the first phase of testing of the step-stress groups at 50 and 70°C were also analyzed to estimate the values of t_0, τ, and t_c.

These data are plotted as a function of reciprocal temperature in Fig. 6. For each temperature, the median value of critical time (the squares) and the standard deviation (the bars) are indicated. The large variance in t_c at each temperature is obvious. This may be due to large slice-to-slice variation in the data obtained from 16 different slices. Nevertheless, the trend for t_c to decrease at high temperature is quite clear. A linear regression analysis of the data on 73 lasers gave

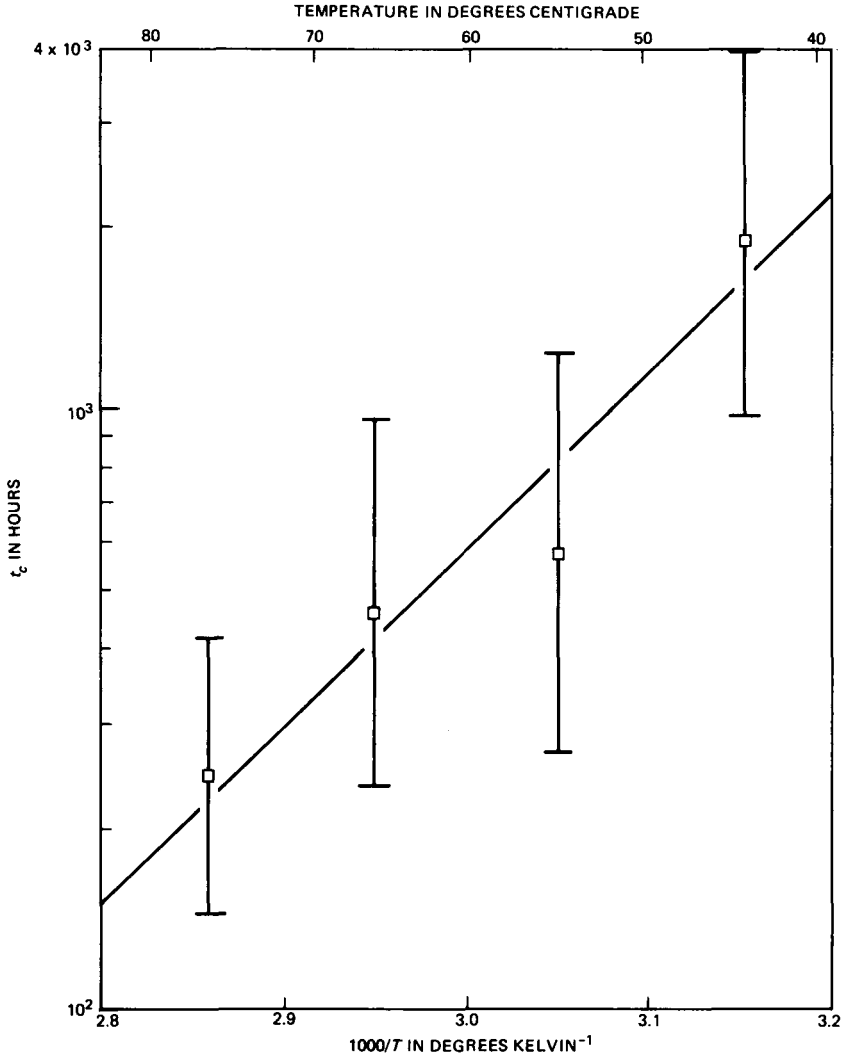

Fig. 6—Data for critical time versus reciprocal temperature, for the saturable current component. The linear regression uses data on 73 lasers.

$$t_c = 7.6 \times 10^{-7}\, e^{E/kT} \text{ hours} \tag{12a}$$

and

$$E = 0.59 \mp 0.06 \text{ eV}, \tag{12b}$$

where the 0.06 eV is the standard deviation. This implies that the time constant for the saturable current has an activation energy that is almost half the value of the main wear-out mechanism. Furthermore, the fit of the linear regression curve to the data is adequate, considering the fact that the curve passes close to the median values at all four temperatures.

Additional observations indicate the following. First, a comparison of the degradation rate in the postknee regime with the strength of the saturable current gave practically no correlation. In other words, the strength of the saturable current was not related in a direct way to the long-term wear-out mechanism. Second, the onset of the saturable current was accompanied by a reduction in the external differential quantum efficiency of the laser. And, finally, the junction voltage at threshold also increased with time in a manner similar to that of the saturable current. Most of these observations are consistent with a model in which the saturable current is associated with an increase in leakage current.[5]

Further clues about the saturable current can be obtained by noting that its activation energy is 0.59 ∓ 0.06 eV. For impurity diffusion in InP, the closest activation energy is that of gold, whose diffusivity is given by the relation[19]

$$D = 1.32 \times 10^{-5} \exp[(-0.48 \mp 0.01)/kT] \text{ cm}^2/\text{s}. \tag{13}$$

Although the activation energies are close, it is not certain whether gold plays a role in the saturable mode of degradation of lasers. The details of such an interaction are even less well understood. We can only conjecture that the complicated reactions involve thermal, electrical, and possibly optical effects.[14,19–28] It is also possible to invoke more complicated models to derive a different value for the activation energy. For instance, formation of dark-spot defects has been described analytically by an exponential function of temperature and a current-squared term.[29] In such a case, the data of Fig. 6 yield an activation energy of 0.24 eV. However, we do not at present have data to justify the use of models that are any more complicated than the simple Arrhenius relation of eq. (12a).

2.4.3 Rate dependence on optical power

A determination of how the degradation rate depends on optical power is necessary for many reasons. From a fundamental point of

view, it is desirable to know whether the long-term wear-out mechanism is being driven predominantly by current (voltage), nonradiative recombination, or the stimulated power. Each of these factors suggests different solutions. From a practical point of view, it is necessary to know how the results of aging lasers under constant power output would compare to the real situation of biasing the lasers at threshold but pulsing them (≈50-percent duty factor) up to the required power output.

As in our methodology for activation energy, we determined the dependence of degradation rate on optical power in the postknee regime by step-power stressing. As shown in Fig. 1, the test was done at constant temperature, i.e., 60°C, and by changing the power between 3 and 5 mW. Furthermore, to safeguard against memory effects, the test was done twice by reversing the power sequence ($3 \rightarrow 5$ and $5 \rightarrow 3$). Finally, in a sequence not shown in Fig. 1, the test is continuing at different power levels (1 and 7 mW), at 60°C.

The dependence of the degradation rate on power $R(P)$ was derived from the step-power experiments by performing a linear regression analysis of the results obtained between any two power levels. This correlation analysis gave the average change in R with power as well as the standard deviation in the estimate of the median value. The results are plotted in Fig. 7. The degradation rate at any power was normalized with respect to its value at 5 mW/facet, i.e., $R(5)$. It is clear from Fig. 7 that as the optical power was reduced, the degradation rate decreased. These results suggest that the dependence of degradation rate on optical power can be represented empirically by the relation

$$R(P) = r_0 + r_1 P, \tag{14}$$

where r_0 is a residual degradation rate which is independent of optical power. For these 1.3-μm lasers, and at 60°C, the value of r_0 was roughly 15 percent of the total degradation rate at 5 mW, as can be seen from Fig. 7.

Equation (14) and the results of Fig. 7 are qualitatively consistent with the results obtained previously.[10,30–32] Except for differences in the functional dependence on power, the results indicate that the degradation rate is comprised of a component r_0 (which may be current driven)[5] and another component $r_1 P$, which is power driven. That this second component is in fact driven by the optical power, and not by current, can be appreciated as follows. At 60°C, the ratio of the drive current at 5 mW to that at 3 mW, $I(5)/I(3)$ is 1.16. Suppose that the observed corresponding change in the ratio of degradation rates of 0.67 is due to current. Therefore, if $R \alpha I^m$, a value of $m = 2.6$ is needed to explain the results. Now this strong dependence of degradation rate

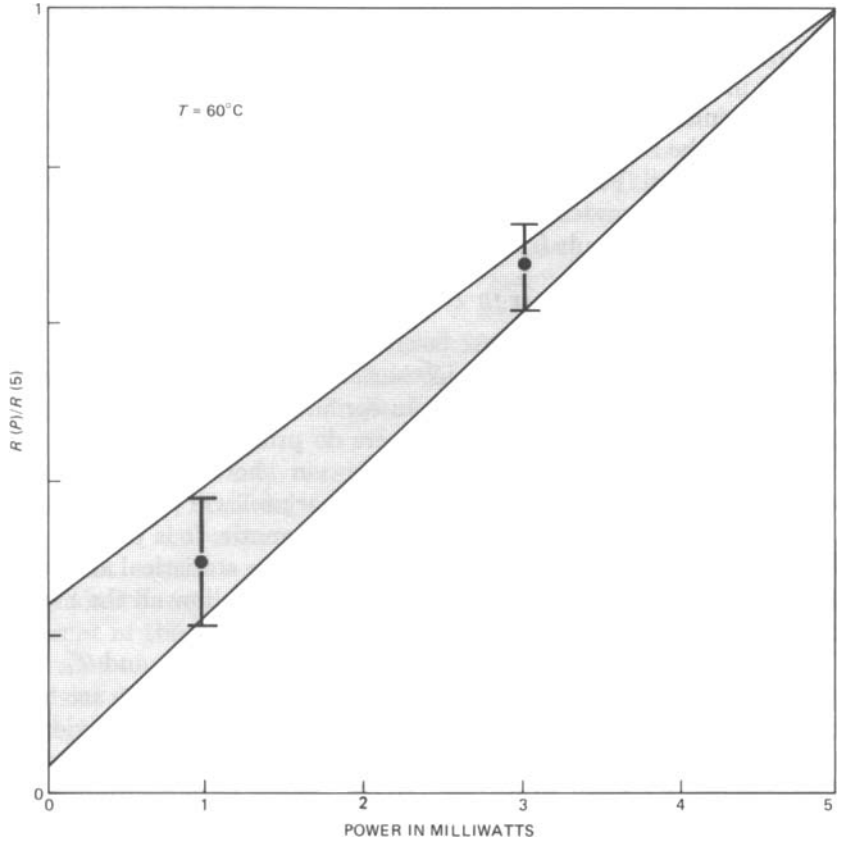

Fig. 7—Dependence of the degradation rate of threshold on optical power measured at 60°C.

on current is inconsistent with our observations on the aging law. A value of $m = 2.6$ leads to a strong superlinearity in the aging characteristics of the lasers. Our data show otherwise. The aging behavior is linear at best and may even have a slight sublinearity in some cases. Hence, a strong current-driven degradation mechanism for our lasers at 5 mW cannot be supported by the observed aging law. Finally, the mode-switching behavior that we sometimes observe, and which will be discussed in subsequent sections, also suggests that the optical fields play an important role in the long-term degradation process.

In summary, the degradation rate at 5 mW per facet and 60°C is made up of two components. One component accounts for ≈15 percent of the total value and may be current driven.[5] The remaining component is driven by optical power. That the dominant degradation process is driven by optical power has at least three justifications. First, for current to explain the degradation results, a strong depend-

ence of degradation rate on current is required. This would imply a superlinearity in the aging law, which is inconsistent with observation. Second, in the step-power experiments at constant temperature, the threshold current is nearly constant. Hence, for significant quantum efficiencies, the residual degradation associated with threshold should remain constant. Finally, the excitation of high-order transverse modes in some degraded lasers suggests a spatially nonuniform degradation, as would result from the optical fields.

2.4.4 Projected operation at 10°C

Out of a total number of 262 lasers tested in this program, more than half (145 lasers) are under isothermal stress test. These groups do not yield activation energy values for individual lasers. The remaining step-temperature-stressed lasers do provide individual activation energies, but only the small fraction shown in Fig. 5 are considered to be sufficiently accurate. The mechanics of projecting the high-temperature data to 10°C becomes problematic. It is possible to treat all the isothermal groups separately, as in the statistical analysis of Amster,[4] or some assumptions can be made that allow all the high-temperature data to be utilized fully.

When a laser is step-temperature stressed between T_1 and T_2, its operation at T_3 can be individually projected. However, there are two sources of error. First, there is the error of estimating its individual activation energy from the measurements at T_1 and T_2. For example, if T_1 and T_2 are 60 and 70°C, respectively, then a 10-percent error in estimating the ratio of degradation rates leads to an error of 0.094 eV in the activation energy. This may seem rather acceptable. However, at 10°C the resulting error in the projected degradation rate is 98 percent, i.e., an order to magnitude larger than the starting measurement error. The reason for this magnification is easy to appreciate in terms of the large "lever arm" involved in such projection.

To minimize the error in projection, the primary source of error associated with activation energy should be minimized. One way to accomplish this is to use the best estimate of activation energy obtained on a fraction of the devices, and use this energy as a "population" parameter to all the lasers. This way, even the lasers being isothermally tested at 40 and 60°C can be projected to 10°C by applying a population activation energy to their measured degradation rates. Our best estimate of activation energy is derived from the results of Fig. 5, in which the median value is 1 eV. Furthermore, 96 percent of the values of activation energy obtained are larger than 0.76 eV and smaller than 1.28 eV.

We have attempted to project the data to 10°C in a manner that will be as representative of the final manufactured product as possible,

which is a difficult task. In the first place, the majority of devices being tested in this program have not been subjected to the rigorous 60°C burn-in screen that the final product will experience. (As described previously, the majority of these devices were subjected to a 50°C/5 mW/100h screen.) This burn-in screen eliminates most lasers with large initial degradation rates (> 50 percent/kh) and large saturable currents. In addition, the present lasers have not been subjected to the purge program, whereas the final product will be.[5] Although the effect of the purge on our projections cannot presently be estimated, it is possible to account for the 60°C burn-in screen. This was done by removing from the statistics all lasers that would fail this burn-in test, had they been subjected to it. This information was available from the degradation of individual devices during the first one hundred hours of stress aging.

When these lasers were subjected to this simulated burn-in screen, and the individual degradation rates projected to 10°C by using a population activation energy, the results are as shown in Fig. 8. For the best estimate of 1 eV for the activation energy, the median degradation rate at 10°C is 4.1×10^{-3} percent/kh. For almost 80 percent of the population, the distribution is fairly well lognormally distributed with a sigma value of 1.8. However, for the remaining 20 percent of the population, which is more rapidly degrading, the curve exhibits truncation. This truncation is due to the 60°C burn-in screen that eliminates rapidly degrading lasers. Further truncation is expected in the final product to be used in the system. The additional truncation results from the added "certification" test to which every laser will be subjected before actually being used.

It is possible to use the projected values of degradation rates at 10°C to estimate the light bulb life of the lasers. Thus, the light bulb Time-To-Failure (TTF) is defined, somewhat arbitrarily, to be

$$\text{TTF} \triangleq 10^5/R(\text{percent/kh}) \text{ hours.} \tag{15}$$

For a linear aging law, eq. (15) implies that the light bulb failure occurs when the threshold current increases by 100 percent. Our transmitter testing on a few lasers, to be discussed elsewhere,[6] shows that (15) is a conservative estimate of light bulb failure. This conservative light bulb TTF definition provides a safety margin to protect against unforeseen functional failures.

Figure 8 shows that for an activation energy of 1 eV, the median TTF at 10°C is slightly greater than 2×10^7 hours. The lower 98-percent confidence limit on activation energy yields a median TTF of 5.7×10^6 hours at 10°C. Also evident in Fig. 8 is the truncation of the distribution curve, which removes devices with relatively short projected lives at 10°C. It has the effect of reducing the rate of early

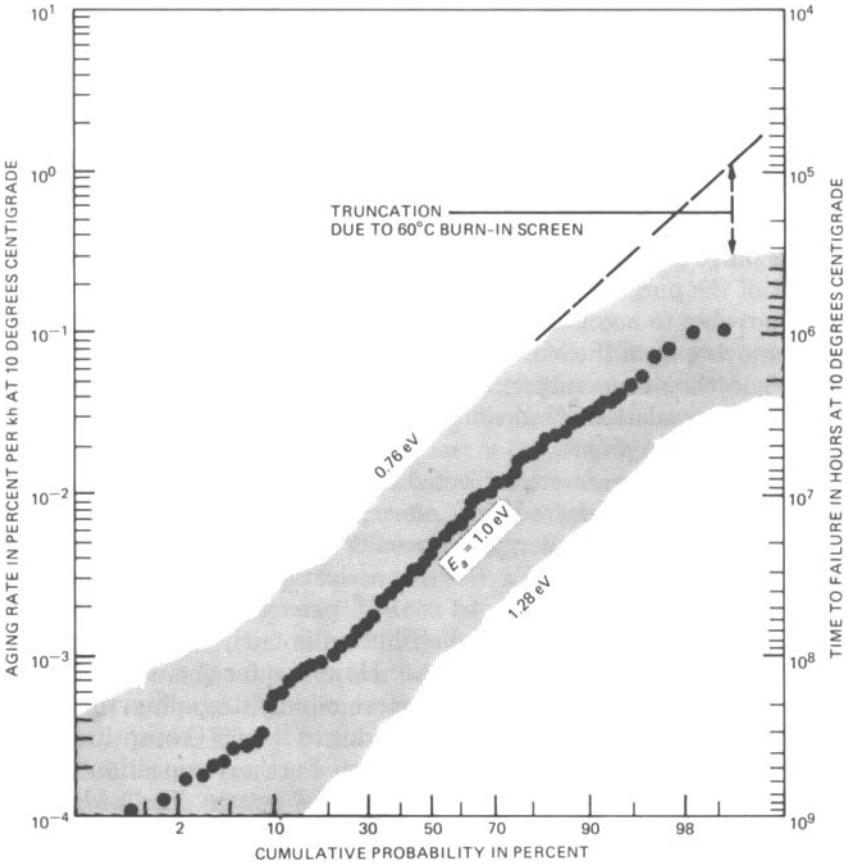

Fig. 8—Degradation rates of individual lasers projected to 10°C using various estimates of activation energy.

failures in the system, below the value expected from the usual log-normal distribution.

2.5 Potential functional failures

Given the relatively long light bulb lifetimes predicted for the 1.3-μm laser at 10°C, it seems prudent to surmise that if and when failures occur, they will be due to operational malfunctions. These potential malfunctions were mentioned in Section 2.1 and include, among other things, change in extinction ratio, excitation of high-order transverse modes, spectral splitting, self-induced pulsations, and fiber-to-laser coupling instabilities in the laser package. Given the incomplete state of our knowledge of these mechanisms, the ability to predict their occurrence is limited. However, some preliminary information about their rate of occurrence and the impact on transmitter performance is beginning to become available.[6]

The occurrence of functional failures should be viewed initially in the context of the overall number of device hours of testing. Thus, the total number of device hours presently available is $\approx 2.4 \times 10^6$ hours. This covers the whole range of temperatures from 10 to 80°C. It is not known, at present, the extent to which functional failures are accelerated with temperature. However, in terms of light bulb life, with an activation energy of 1 eV, the various testing at different temperatures is equivalent to 9.3×10^8 device hours at 10°C. Hence, for a configuration that uses ≈1000 active lasers, the equivalent time is ≈106 years of system operation at 10°C.

With all the caveats stated above in mind, we can say that there is no available evidence to indicate that functional failures will have a severe impact on system reliability. However, we have identified (in three rapidly degrading lasers that normally would not pass the 60°C burn-in screen) certain anomalies that affect, for instance, the coupling efficiency into the single-mode fiber. Such an example is shown in Fig. 9. The laser had been stressed at 40°C to the extent that its threshold increased by ≈50 percent. After this amount of degradation, the laser power output at 10°C, as monitored by the back-face detector, showed an abrupt change in quantum efficiency at a current 9 mA above threshold, as shown in Fig. 9a. The output from the single-mode fiber is even more remarkable. For currents between the threshold value (43 mA) and 52 mA, the fiber coupling efficiency was very low. However, the coupling efficiency above 52 mA increased, as evident from Fig. 9a. The optical spectrum, when measured through the single-mode fiber, is shown in Fig. 9b. For wavelengths between 12,850 and 12,875Å, there was evidence of another family of longitudinal modes that are closely spaced to the main optical mode. It was therefore concluded that this optical spectrum was comprised of a fundamental and a high-order transverse mode whose coupling efficiency to the single-mode fiber was rather low.

There was also direct evidence that the initially fundamental TE_0 (Transverse Electric) mode could change, in some rapidly degrading lasers, to a high-order TE_n mode. An example of an extreme case is shown in Fig. 10. Initially, the far-field emission pattern indicated a well-behaved fundamental transverse mode. After accelerated aging, which produced a 70-percent increase in threshold, the far-field pattern became as shown in Fig. 10. (The final far-field measurements were made by R. T. Ku, who used a numerical aperture of 0.2. The initial far-field measurement used a numerical aperture of 1, which may have lead to some smoothening of the fine structure in the radiation pattern.) The dominant mode in the degraded laser became a TE_1 transverse mode. However, optical spectral measurements of the same laser indicated the presence of four distinct families of

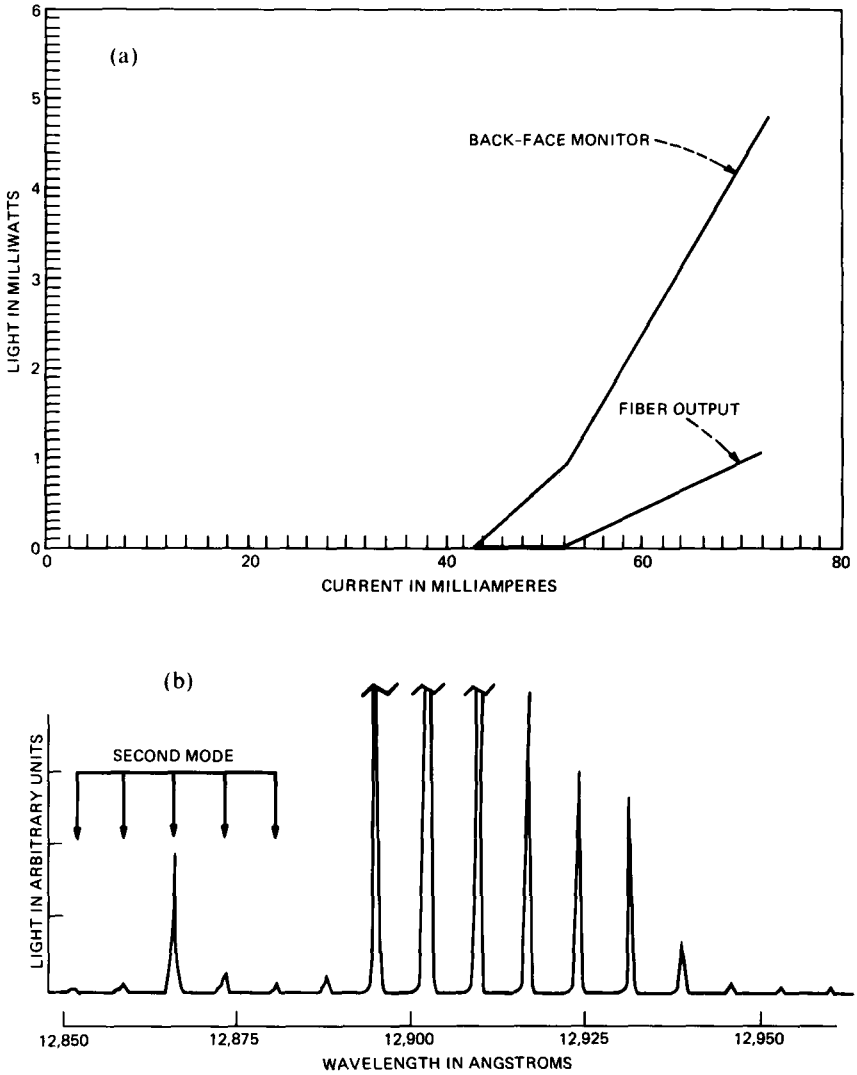

Fig. 9—An example of potential malfunction of a degraded device measured at 10°C. (a) Light-current characteristic and (b) spectrum measured through the optical fiber at 5 mW.

longitudinal modes. Hence, in addition to the TE_0 and TE_1 modes, there were two TE modes that were not very distinct in Fig. 10. In general, the high-order modes encountered after degradation were odd-numbered and TE polarized. Inspection of the mirror facets indicated no obvious erosion. Therefore, the degradation process seemed to be in the bulk of the active regions, and may be similar to the "spottiness" observed in degraded GaAs lasers.[33]

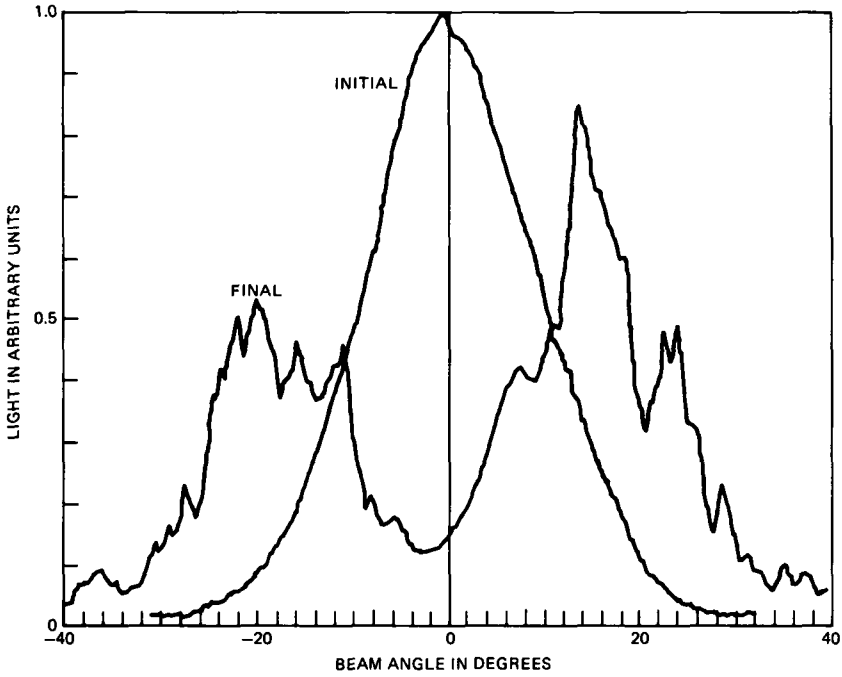

Fig. 10—An example of extreme distortion in the far field of a degraded laser obtained from slice C of Table III.

Further diagnostic tests were performed on selected lasers that exhibit light-current nonlinearities, additional spectral modes, and reduced fiber coupling. In all such cases, the width of the active region was found to exceed the 1- to 1.7-μm target value. For instance, the laser whose characteristic is shown in Fig. 9 was obtained from slice N of Table III in Appendix B. Lasers from this slice had an unusually high rate of incidence of a secondary family in the optical spectra, indicating high-order transverse modes. Several lasers from this slice had their mirrors etched in a potassium-ferrocyanide solution. Subsequent measurements of the etched mirrors in a Scanning Electron Microscope (SEM) indicated that the width of the active region for slice N was $\approx$2.5 μm, i.e., about 1 μm larger than the desired value. The laser whose far-field pattern was shown in Fig. 10 deviated even further from the nominal value. Its active region was $\approx$4 μm wide. In all cases of clear evidence of high-order modes, the width of the active region exceeded 2 μm. The intriguing aspect of this result was that all the lasers initially had a fundamental transverse mode. The high-order modes developed in degraded lasers if the active region exceeded $\approx$2 μm.[32] Therefore, better production or screening control should eliminate these potentially malfunctioning lasers. Such screening tests

may involve freedom from "kinks" in the light-current curves up to 10 mW, noninvasive stripe width measurements, far-field radiation patterns, and spectral measurements. In addition, it is possible to obtain a direct measure of stripe width by performing etching and SEM measurements on the nearest-neighbor laser to that intended for system use.[34]

It is clear that the above examples are but a few of the many ways in which lasers could fail functionally. So far, we have encountered only two degraded (out of 262) lasers that developed weak (−90 dBm) self-induced pulsations occurring at 2.4 and 3.1 GHz, respectively. This is at variance with the high rate of incidence of self-induced pulsations in proton-bombarded GaAs lasers.[35] The reason may be due to the strong index guiding properties of buried heterostructure lasers.[36] However, this by no means exhausts all the possibilities of functional failures, which are actively being investigated.[6]

III. CONCLUSION

In this phase of prequalification reliability program we have defined both the reliability potential as well as the testing methodology of 1.3-μm lasers. There are stringent reliability conditions imposed on all components used in submarine cable systems. This requires accurate knowledge of the fundamental reliability parameters that influence long-term projections. Our experiments on unpurged lasers revealed short-term saturable effects as well as long-term degradation. By carefully choosing experiments in the laser program, we have been able to establish a population value for the activation energy of 1 eV for the long-term degradation process. Furthermore, 96 percent of the measured values of the activation energy are between 0.76 and 1.28 eV. These activation energies allow projections to 10°C that imply a most probable median time to failure in excess of 2×10^7 hours, for light bulb life. By the same token, with 98-percent confidence level, the median time to failure at 10°C is greater than 5.7×10^6 hours. These projections are based on devices that have been subjected to a short (100-hour) screen at 60°C, which eliminates most potential early failures. An additional long-term screen at 60°C is planned for the laser certification program. Both screening operations lead to a severe truncation of the distribution curve for short-lived devices. This reduces the early failure rate below the value expected from the usual lognormal distribution.

The initial phase of this program studied in detail the light bulb life of 1.3-μm lasers and determined that it is adequate for submarine cable application. It is obvious that there is another class of failures that can have an adverse impact on laser system performance. For instance, nonthermally activated failure mechanisms or early random

failures may occur in some devices. These potential failures we expect to reduce to a minimum by subjecting the lasers to a severe purge program.[5] Another class of failures is related to operational malfunctions. This class is currently being studied actively and the information is quite preliminary. However, there are no indications, so far, to lead us to believe that operational failures should significantly alter our conclusions about the utility of the 1.3-μm laser for submarine cable use.

IV. ACKNOWLEDGMENTS

The authors are indebted to the members of the "reliability committee" for long and useful discussions. Among these are S. J. Amster, C. E. Barnes, P. Bossard, M. Choy, R. L. Easton, H. E. Elder, R. L. Hartman, J. H. Rowen, M. Tortorella, and C. B. Swan. The authors are also grateful to F. R. Nash, R. G. Smith, A. E. Bakanowski, and E. I. Gordon for a critical reading of the manuscript.

REFERENCES

1. M. Hirao et al., "Fabrication and Characterization of Narrow Stripe InGaAsP/InP Buried Heterostructure Lasers," J. Appl. Phys., *51* (August 1980), pp. 4539–40.
2. K. Mizuishi et al., "Accelerated Aging Characteristics of InGaAsP/InP Buried Heterostructure Lasers Emitting at 1.3 μm," Jap. J. Appl. Phys., *19* (July 1980), pp. 429–32.
3. K. Mizuishi et al., "Reliability of InGaAsP/InP Buried Heterostructure Lasers," Jap. J. Appl. Phys., *21*, Supplement 21-1 (1982), pp. 359–64.
4. S. J. Amster, unpublished work.
5. F. R. Nash et al. "Implementation of the Proposed Reliability Assurance Strategy for an InGaAsP/InP, Planar Mesa, Buried Heterostructure Laser Operating at 1.3 μm for Use in a Submarine Cable," AT&T Tech. J., this issue.
6. C. E. Barnes and W. Smith, unpublished work.
7. D. S. Peck and C. H. Zierdt, Jr., "The Reliability of Semiconductor Devices in the Bell System," Proc. IEEE, *62* (February 1974), pp. 185–211.
8. G. A. Dobson and B. T. Howard, "High Stress Aging to Failure of Semiconductor Devices," Proc. Seventh Nat. Symp. Rel. Qual. Contr. Electron. (1961), pp. 262–72.
9. Y. Horikoshi, T. Kobayashi, and Y. Furukawa, "Lifetime of InGaAsP-InP and AlGaAs-GaAs DH Lasers Estimated by the Point Defect Generation Model," Jap. J. Appl. Phys., *18* (December 1979), pp. 2237–44.
10. H. Imai et al., "Accelerated Aging Test of InGaAsP/InP Double-Heterostructure Laser Diodes With Single Transverse Mode," Appl. Phys. Lett., *38* (January 1981), pp. 16–7.
11. R. G. Smith, private communication.
12. G. H. B. Thompson, "Temperature Dependence of Threshold Current in (GaIn)(AsP) DH Lasers at 1.3 and 1.5 μm Wavelengths," IEE Proc. I, Solid State Electron Dev., *128* (January 1981), pp. 37–43.
13. G. H. B. Thompson and G. D. Henshall, "Nonradiative Carrier Loss and Temperature Sensitivity of Threshold in 1.27 μm (GaIn)(AsP)/InP D. H. Lasers," Electron. Let., *16* (January 1980), pp. 42–4.
14. N. K. Dutta and R. J. Nelson, "Gain Measurements in 1.3 μm InGaAsP-InP Double Heterostructure Lasers," IEEE J. Quantum Electron., *QE-18* (January 1982), pp. 44–9.
15. M. Yano, H. Imai, and M. Takusagawa, "Analysis of Electrical, Threshold, and Temperature Characteristics of InGaAsp/InP Double-Heterojunction Lasers," IEEE J. Quantum Electron., *QE-17* (September 1981), pp. 1954–63.
16. A. Sugimura, "Band-to-Band Auger Recombination Effect on InGaAsP Laser Threshold," IEEE J. Quantum Electron., *QE-17* (May 1981), pp. 627–34.
17. Y. Horikoshi and Y. Furakawa, "Temperature Sensitive Threshold Current of

InGaAsP-InP Double Heterostructure Lasers," Jap. J. Appl. Phys., *18* (April 1979), pp. 809–15.
18. W. C. Ballamy and L. C. Kimerling, "Premature Failure in Pt-GaAs IMPATT's—Recombination-Assisted Diffusion as a Failure Mechanism," IEEE Trans. Electron. Dev., *ED-25* (June 1978), pp. 746–52.
19. S. I. Rembeza, "Diffusion of Au in InP Single Crystals," Sov. Phys. Semicond., *3* (October 1969), pp. 519–20.
20. A. K. Chin et al., "Cathodoluminescence Evaluation of Dark Spot Defects in InP/InGaAsP Light Emitting Diodes," Appl. Phys. Lett., *41* (September 1982), pp. 555–7.
21. I. Camlibel et al., "Metallurgical Behavior of Gold-Based Ohmic Contacts to the InP/InGaAsP Material System," J. Electrochem. Soc., *129* (November 1982), pp. 2585–90.
22. O. Ueda et al., "Mechanism of Catastrophic Degradation in InGaAsP/InP Double-heterostructure Light Emitting Diodes and GaAlAs Doubleheterostructure Light Emitting Diodes Applied With Pulsed Large Current," J. Appl. Phys., *53* (December 1982), pp. 9170–9.
23. O. Ueda et al., "Transmission Electron Microscope Observation of Dark-Spot Defects in InGaAsP/InP Double-Heterostructure Light-Emitting-Diodes Aged at High Temperature," Appl. Phys. Lett., *36* (March 1980), pp. 300–1.
24. S. Yamakoshi et al., "Reliability of High Radiance InGaAsP/InP LED's Operating in the 1.2–1.3 μm Wavelength," IEEE J. Quantum Electron, *QE-17* (February 1981), pp. 167–73.
25. S. D. Hersee, "Long Lived High Radiance LEDS for Fiber Optic Communications Systems," Digest Seventh Int. Electron Dev. Meeting, 1977, pp. 567–70.
26. K. Wakita et al., "Transmission Electron Microscope Observation of Dark Defects Appearing in InGaAsP/InP Double Heterostructure Lasers Aged at Accelerated Operation," Appl. Phys. Lett., *40* (March 1982), pp. 525–7.
27. K. Ishida, T. Kamejima, and Y. Matsumoto, "Lattice Defect Structure of Degraded InGaAsP/InP Double-Heterostructure Lasers," Appl. Phys. Lett., *40* (January 1982), pp. 16–7.
28. S. Komiya et al., "Optically Induced Glide Motion of Misfit Dislocations in InP/$In_{1-x}Ga_xAs_{1-y}P_y$ Double Heterostructure," J. Appl. Phys., *54* (February 1983), pp. 1058–61.
29. S. Yamakoshi et al., "Degradation of High Radiance InGaAsP/InP LEDs at 1.2–1.3 μm Wavelength," IEDM Tech. Digest, Washington, D.C., 1979, pp. 122–5.
30. K. Hori, H. Imai, and M. Takusagawa, "Long-Lived GaAlAs-GaAs DH Laser Diodes for Optical Fiber Communications," Fujitsu Sci. Tech. J., *15* (December 1979), pp. 95–109.
31. H. Ishikawa et al., "Accelerated Aging Test of Ga_{1-x} Al_xAs DH Lasers," J. Appl. Phys., *50* (April 1979), pp. 2518–22.
32. K. Mizuishi et al., "Reliability of InGaAs/P/InP Buried-Heterostructure 1.3 μm Lasers," IEEE J. Quantum Electron., *QE-19* (August 1983), pp. 1294–301.
33. H. Kressel and J. K. Butler, *Semiconductor Lasers and Heterojunction LEDs*, New York, NY: Academic Press, 1977.
34. C. B. Swan, private communication.
35. T. L. Paoli, "Changes in the Optical Properties of CW (AlGa)As Junction Lasers During Accelerated Aging," IEEE J. Quantum Electron., *QE-13* (May 1977), pp. 351–9.
36. B. W. Hakki, "Instabilities in Output of Injection Lasers," J. Appl. Phys., *50* (September 1979), pp. 5630–7.

APPENDIX A

Aging and Testing Facilities

The variety of testing conditions required that a large quantity of lasers operating at various temperatures must be accommodated at the same time. The following criteria governed the design of the 1400 Continuous Wave (CW) and 120 pulsed aging sites for packaged 1.3-μm lasers. We will demonstrate in this Appendix that we have con-

structed a test facility which meets the criteria listed below, particularly the third item.

1. In-place testing and aging—For efficient aging of a large number of devices, in-place testing becomes mandatory.

2. Automated optical and electronic measurements—The large amount of data taken requires that all of the optical, as well as the electronic, measurements are made in situ and under computer control.

3. Precision and stability—The precision and stability of the measurements must allow the laser characteristics to be projected accurately to 200,000 hours, based on less than 10,000 hours of data on each laser. With proper balance of all design factors, we can make the most efficient use of an expensive facility.

A.1 Description of facilities

The SL laser CW aging facility consists of aging cabinets; an uninterruptible (battery reserve) power system; a master computer; and multiplexing for the electrical, optical, and radio frequency spectrum measuring equipment. Twenty different temperatures (70 lasers each) can be controlled simultaneously. All testing is performed in place and is initiated by a master computer. The operating currents of these lasers have temperature sensitivities in the range of 0.5 to 2 mA/°C, depending on the laser and the temperature. Approximately 0.1-mA stability is needed to take data in less than 10,000 hours and project it to 200,000 hours with greater than 98-percent confidence that the current will not double. We therefore made a preliminary estimate that ±0.05°C temperature control was necessary for testing InGaAsP lasers. The exact details depend on the laser and the conditions at which it is aged.

During aging, the computer-controlled temperatures of the devices are held at ±1°C within the range of 10 to 90°C. The lasers are aged at a current level that is continuously adjusted, using analog circuitry, to provide constant power output. This power output is typically 5 mW per facet, which is the system operating power level. Four times a day, the Light-Current-Voltage-Temperature (L-I-V-T) is measured to ensure the integrity of the automatic feedback circuitry and temperature control.

Every 50 hours, the computer initiates L-I-V in-place tests on each laser. During the test, the relative temperature is held to ±0.05°C of the nominal aging temperature. The absolute temperature is known to within 0.5°C. The current on each device is decreased in increments of ≈0.4 mA from its operating current down to zero. At each current level, the light from the fiber (L_F), light on the rear-face detector (L_R), current, and voltage are measured. From this set of measurements are derived the IdV/dI, I^2d^2V/dI^2, dL/dI, d^2L/dI^2 curves for each device

at a particular temperature and time. The derivatives for light are computed only for the rear-face light. The data are analyzed and stored by the computer to give information about threshold, modulation current, nonradiative or leakage current, kinks in the LI curve that may indicate high-order transverse modes, diode resistance, and spontaneous emission at threshold that can affect the extinction ratio. The fiber-to-rear-face power ratio gives the fiber coupling efficiency (η_c).

The test facility can also provide tests relevant to possible operational failures of the laser. For instance, the optical spectrum of the light launched into the single-mode fiber is measured. The data are digitized and stored in the computer. Spectral splitting, mode broadening, or excitation of an additional family of longitudinal modes, though rare, have been detected from these data.

The existence of self-induced pulsations or excessive noise is monitored by analyzing the microwave spectrum of the laser output from 100 kHz to 3.5 GHz. Depending on the frequency and intensity of the microwave noise, the error rate in the optical link could increase above the maximum allowed limit of 10^{-9}/s.

An auxiliary package pulse aging facility consists of 120 positions capable of modulating the laser using pseudorandom pulses at data rates to 300 Mb/s. In addition, all the tests described for the CW facility are made for the pulse system as well. The controller is a separate desk top computer separate from the one used for the CW facility.

The main purpose of pulse aging is to compare the pulsed aging rates with the CW aging rates. In the qualification program about 10 percent of the lasers to be aged will be aged under pulsed conditions to assure that no degradation mechanism unique to pulsed operation exists.

A.2 Performance

Because of the high temperature coefficient of laser current at a fixed light output, temperature variations are a major contributor to variations in laser current. In our aging racks, we have achieved a day-to-day control of the relative temperature of ±0.05°C during measurements of laser characteristics. We have measured the long-term standard deviation of the laser current (I_5) at a fixed light output of 5 mW and determined it to be 0.10 mA. This value, (I_5), is included with the short-term and long-term measurement accuracies of important laser parameters in Table II. Threshold current (I_{th}), which is derived digitally from the maximum in d^2L/dI^2, has a long-term standard deviation of 0.20 mA. The mean value for the short-term standard deviation for I_5 was 5 microamperes, a factor of 20 less than the long-term value. This result is consistent with our original estimate that

Table II—Measurement accuracy

Parameter	Units	Short-Term Standard Deviation	Long-Term Standard Deviation
I_{th}	mA	0.1	0.20
$I_{5(mW)}$	mA	0.005	0.10
dI_{th}/dt	mA/kh	—	0.04
dI_5/dt	mA/kh	—	0.02
$\eta_c = L_F/L_R$*	dB	0.01	—
T	°C	0.008	0.036

* L_F is the light from the fiber and L_R is the light from the rear face of the laser.

temperature control would dominate the long-term stability measurements of threshold and drive current on these lasers.

The aging rates of threshold and 5-mW operating currents are two of the most important parameters that we study. If the linear law of eq. (6) in the main text is assumed, the Gaussian statistics for deriving the aging rate from estimates of measurement variance can be modeled. The results depend on the frequency and distribution of the measurements over a given time interval. For the 0.1-mA, long-term standard deviation for I_5 given in Table II and 60 measurements made uniformly over 3000 hours, the uncertainty in the aging rate would be 0.02 mA/kh. We also get this value for the standard deviation of the aging rate, R for I_5 in Table II, which is the average of many least squares fits to $I(t)/I_o = 1 + Rt$. The data used were from devices with 2000 to 4000 hours of stable aging characteristics at 12 and 50°C and no obvious knee characteristic.

We will be able, assuming that the linear model continues to provide an upper bound to the extrapolated operating current, to extrapolate with a few milliamperes of uncertainty the operating current to 200,000 hours at any temperature with 3000 hours of data. In particular, we can certify each laser package for current stability by operating it at 10°C for 3000 hours. In addition, each laser chip will have seen a high-temperature aging during a purge that is equivalent to tens of thousands of hours of system operation at 10°C. After packaging, the laser will again see the temperature accelerated equivalent of at least one million system hours during a 60°C part of the package certification.

Our situation in fiber coupling measurements and measurements of the stability of the test apparatus is not yet firmly established. It is desirable that we have an engineering safety factor on the fiber coupling stability verifiable on individual lasers by temperature acceleration. The uncertainty in documenting this stability is related to the early stage of this phase of the program. The main concern in packaged lasers is related to the potential for mechanical relaxation phenomena causing changes in the fiber coupling. Our observation to date has been that the rate of change of fiber coupling decreases with time; i.e.,

the rate is sublinear. Therefore, our initial measurements will provide an upper bound on the linear decoupling rate.

Our short-term measurement error for fiber coupling is given in Table II. The short-term value is small enough to make 3,000-hour coupling projections to 200,000 hours with only a few percent uncertainty in the coupling. As in the case of current stability, the assumption is made that a linear fit is an upper bound on the aging rate. This assumption will be checked on individual lasers.

We do not yet have data on the long-term standard deviation for fiber coupling. The temperature coefficient is 0.02 dB/°C, three to four times smaller than the laser current temperature coefficient. Therefore, we expect the long-term measurement error to be dominated by the repeatability of the alignment of our computer-controlled optical multiplexer. The short-term measurement error, 0.01 dB, is a measure of this repeatability.

In conclusion, at AT&T Bell Laboratories we have built and tested aging facilities that meet the criteria outlined at the beginning of this section. Assuming a linear model, we can project, with a few milliamperes uncertainty, laser 5-mW operating current stability to 200,000 hours or 24 years with 3000 hours of data. This can be done at any of our operating temperatures, including the 10°C system operating temperature. Our short-term fiber coupling efficiency measurements indicate similar accuracies and projection test times for fiber coupling efficiency measurements. We expect our long-term accuracy to be compatible with the required 200,000-hour extrapolations.

APPENDIX B

Design of the Reliability Experiments

All lasers are aged in packaged form. Two types of packages are used. The first is the so-called multimode package, which uses a Ge detector to monitor the power output from the back face of the laser. This package also uses a multimode fiber to couple the power output from the front face of the laser. The second type of package is the so-called single-mode package, in which the output from the front face is coupled into a single-mode fiber. It uses an InGaAs PIN detector to monitor the power output from the back face of the laser. The multimode package is easier to make and couples more effectively into high-order transverse modes. Therefore, the multimode package is a useful vehicle for some diagnostic purposes. On the other hand, the single-mode package is ultimately the final design configuration that provides information about the stability of the coupling of the fiber to the laser. Out of a total of 262 lasers tested in this reliability program, 129 are in single-mode packages and 133 are in multimode packages.

Table III—1.3-μm laser and slice allocation

Slice Number	Group 1		2		3		4		5		6		7		8	
	Test: Step		Step		10°C		60°C		40°C		Step		Step		30°C	
	Package* M	S	M	S	M	S	M	S	M	S	M	S	M	S	M	S
A	1															
B	8		1													
C	5		1													
D	6		6												2	3
E			10			5						4		1		
F						2		5		1						2
G					4	2					3	1				
H					7		6			9						4
I							10		5	3						
J											2	2		6		
K											4	1	5			
L							5	2	2	3						4
M							6		6							
N							6			5						4
O			2						6							
P												5		3		6
Q												8		7		
R											4	3		5		
S														6		
T					5									4		
U					4	1										
V						3								3		
W						3										
X					3	1										

* M—Multimode. S—Single mode.

The 262 lasers being tested are divided into eight groups listed in Table III. Four of the groups (1, 2, 6, and 7) are step stressed in temperature and power. The remaining four groups (3, 4, 5, and 8) are isothermally tested at 5 mW and the temperatures indicated in Table III. Groups 1 and 2 are stepped in temperature and power according to the sequence shown schematically in Fig. 1. Groups 6 and 7 are step-temperature stressed at 5 mW in the sequence shown in Fig. 2. In addition, to the extent possible, Groups 6 and 7 contain lasers obtained from split-lot slices, as indicated in Table III. This is done to provide a degree of homogeneity in the results between the two groups. By the same token, Groups 4 and 5, isothermally tested at 60 and 40°C, respectively, also involve split-lot slices. This attempt to homogenize the isothermal groups is mandatory for a proper interpretation of the results. The reasons for this are obvious. Within each slice, the laser-to-laser variability in degradation rate is about an order of magnitude. In addition, slice-to-slice variability can be two orders of magnitude.

Hence, to measure the temperature acceleration of degradation between 40 and 60°C, which is expected to be one order of magnitude, is very difficult if each individual population has a spread of three orders of magnitude. Hence, to compensate for this large variance within each test group, an attempt to homogenize comparable groups is made by selecting devices from the same slices. This provides by no means a perfect solution, but is an attempt to ameliorate an otherwise intolerably large variation.

Groups 3 and 8 of Table III are also isothermally tested at 10 and 30°C, respectively. Group 8 attempts to match devices from Groups 4 and 5. The choice of 30°C testing provides a check of the Arrhenius relation as obtained from isothermal testing.[4] The testing time at 30°C, required to establish valid long-term trends, is unfortunately very long, $\geq 10^4$ hours. Hence, at the present time, the 30°C testing data are too preliminary to provide accurate quantitative information. On the other hand, the 10°C isothermal group contains samples from various slices that are being tested at high temperatures, either step stressed or isothermal. The utility of the 10°C test group is to provide, in the long term, a correlation between high-temperature test data and the system operating temperature. In addition, it is a necessary experiment that would uncover any laser performance malfunctions that may be unique to 10°C operation. So far, no fundamental problems have been encountered that are peculiar to 10°C operation.

Finally, it is seen that Table III lists lasers obtained from 24 slices. This represents a fairly wide cross section of material made from early development (e.g., slices A, B, C, and D) to slices made under strict production control environment (e.g., slices T, U, V, W, and X). The basic laser design is almost unchanged throughout. The fact that a good performance record can be demonstrated for lasers, going from development to production, attests to the basic viability of this device. It should also be emphasized that the number of lasers associated with each slice in Table III does not represent the total number from each slice. The lasers used in this reliability program represent only a portion of the total devices. Other lasers are used in diagnostic evaluation, laser-transmitter evaluation, purge development, other experiments, etc.

AUTHORS

Thomas F. Eltringham, A.A.S. (Electronics Engineering Technology), 1967, DeVry Institute of Technology; AT&T Bell Laboratories, 1967—. After joining AT&T Bell Laboratories, Mr. Eltringham was involved in the design of test equipment for phase-array radars. He then worked on the design, testing, and reliability studies of light-emitting diodes and lasers. He is currently involved in laser reliability studies for undersea applications.

Phillip E. Fraley, B.S. and M.S. (Engineering Physics), 1962, Ph.D. (Physics), 1966, The Ohio State University; Aerospace Research Laboratory (USAF), 1966–1969; AT&T Bell Laboratories, 1969—. At AT&T Bell Laboratories, Mr. Fraley has worked on the design and characterization of more than 60 Light-Emitting Diodes (LEDs). He then worked on the reliability and characterization of GaAlAs lasers. Mr. Fraley's recent work has been the use of specialized computer hardware to obtain precise measurements of the optoelectronic parameters needed to quantify InGaAsP laser stability.

Basil W. Hakki, B.S.E.E., 1957, M.S., 1958, Ph.D., 1960 (Electrical Engineering), University of Illinois; AT&T Bell Laboratories, 1963—. After joining AT&T Laboratories, Mr. Hakki was involved in the design and analysis of GaAs two-valley microwave oscillators. He then worked with III–V LEDs and lasers. His work on GaAs double heterostructure injection lasers covered many aspects of the laser, including reliability, device design for CW and high-power operation, and device physics. He is currently involved in the study of quaternary lasers.